 CMES, vol.91, no.6, pp.425-444, 2013

Characterization and modeling of the multiscale pore structures for porous materials

X.F. Guan[1], **X. Liu**[2], **J.Z. Cui**[3]

Abstract: In this paper, a stochastic geometrical modeling method for reconstructing three dimensional multiscale pore structures of porous materials is presented. In this method, the pore structure in porous materials is represented by a random but spatially correlated pore-network, in which the results of the Mercury Intrusion Porosimetry (MIP) experiment are used as the basic input information. Beside that, based on the Monte Carlo techniques, an effective computer generation algorithm is developed, and the quantities to evaluate the properties of porous materials are defined and described. Furthermore, numerical implementations are conducted based on experimental data afterwards. This method can be used to generate multiscale pore structure models of a wide class of porous materials.

Keywords: Multiscale pore structure, Stochastic pore-network model, Monte Carlo techniques, Take-and-place method.

1 Introduction

Many types of materials, including ceramics, concrete, asphalt, soils and rocks, are categorized into porous materials with pores either artificially made for a specific purpose or naturally formed by a physical process. Such materials tend to have very small pores, which may be open and connected, or closed, and are often subjected to thermal or chemical attack at the internal boundaries formed by pores as well as the external boundaries.

[1] Department of Mathematics, Tongji University, Shanghai 200092, China.
[2] Department of Geotechnical Engineering, Tongji University, Shanghai 200092, China. Corresponding Author, Email: xian.liu@tongji.edu.cn
[3] Academy of Mathematics and System Science, Chinese Academy of Sciences, Beijing 100190, China.

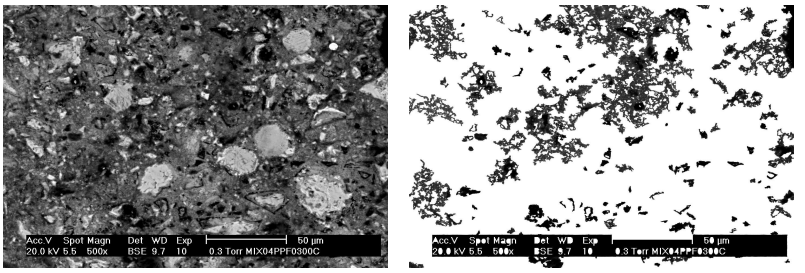

(a) (b)

Figure 1: SEM image and grey scale image of cement-based material [Liu (2006)]

Getting insight into the pore structure of porous materials is a long time effort of researchers and engineers, as it is now widely accepted that the pore structure of porous materials is one of the key issues which determine materials' macroscopic properties including permeability, diffusivity [Liu, Zeiml, Lackner, and Mang (2010)], mechanical behavior [Dong and Atluri (2012); Yan, Zhang, Ye, and Yu (2010); Jr., Sladek, Sladek, Zmindak, and Medvecky (2012); Han, Cui, and Yu (2010)], or heat transfer [Yang, Cui, Nie, and Ma (2012); Han, Cui, and Yu (2009)]. For example, in case of high-temperature loading of concrete structures, vaporization of physically and chemically bound water results in an increase of pore pressure. The low transport ability causes spallation of near surface concrete layers. This pressure driven transport of water vapor is commonly described as the governing parameter by Darcy's law with the permeability [Zeiml (2008)]. To further understand and model these macroscopic properties, plenty of effort has been focused on modeling the pore structure to adequately describe the pore geometrical and topological properties of the real porous materials. The related attempts have been conducted both experimentally and theoretically, in which each method shows its limitation [Liu (2006)].

In this regard, attempts to characterize and reconstruct the pore structure via experiments have been made for a long period of time. The knowledge about pore structure of porous materials deeply depends on the development of experimental techniques. Plenty of technical methods have been employed to measure the microstructure. Among these techniques are Mercury intrusion porosimetry (MIP), Brunauer, Emmet and Teller isotherm (BET) / Nitrogen desorption, Scanning electron microscopy (SEM) image analysis, X-ray scattering (SAXS), Nuclear magnetic resonance (NMR) / Freezing point depression. As far as the pore structure of porous materials is concerned, which consists of its geometrical and topological properties: the shape, volume of pores and its location, the above techniques normally give access to the pore-size distribution and the total pore volume, but

may not identify the connection and location of the pores, thus building up different pore arrangements with different macroscopic input parameters becomes very important.

Based on the above experimental techniques, the reconstruction of pore structure has been mostly performed by two different models, which are digital images analysis method and MIP data analysis method. Digital image analysis method allows us to determine geometrical properties of the three dimensional pore network by processing data of two dimensional random sections [Dullien (1979)] with the aid of the principle of quantitative stereology [Underwood (1970)], and estimate topological properties of the interconnected pore structure by analyzing data of serial sections. Algorithms of reconstruction of three dimensional pore network from data of two dimensional pore features of serial sections [DeHoff, Aigeltinger, and Craig (1972)] have been developed for the simultaneous determination of both topological and geometrical properties of porous materials [Garboczi and Bentz (1996); Sadouki and Mier (1997); Ye, Lura, and Breugel (2006)]. Moreover, Mercury Intrusion Porosimetry (MIP) is the fastest method of determining the capillary pressure curves, in which information about a wide range of pore sizes is embedded. Therefore, MIP is the most important method of analyzing the pore structure for a wide variety of porous material. In the form of pore volume cumulative curve, many researchers have developed some reconstruction algorithms to simulate the pore structure, in which the pore structure is idealized as a network consisting of regular-shaped pore bodies and pore throats [Mata, Lopes, and Dias (2001); Tsakiroglou and Payatakes (1998)].

However, according to the pore sizes of porous materials, which normally ranges from 1 nm to 1mm, it must be noted that the above techniques have their own application limitations. It is difficult to generate geometric and physical samples due to huge workload. And another significant difficulty in using the above pore-network models in a quantitative predictive sense lies in choosing the geometric shapes, sizes, locations, and orientations of the pore bodies and throats so that the amount of detail in the description of the pore space geometry is sufficient to make accurate prediction of macroscopic properties.

In the present work, we develop a multi-scale modeling method to treat a pore structure as a three-dimensional random, and use the MIP experimental results as the basic input. The algorithm takes on the following merits: (1) Suiting to generating random samples with larger length-scale gap due to using ε-size random distribution model. (2) The generated samples have better randomness, which means that the shape, size, locations, and orientations of the pore bodies and throats are completely implemented. (3) To be able to generate not only the models with uniform and norm random distributions, but also those with specified distributions obtained

from MIP experiment.

The remainder of this paper is organized as follows: In Section 2, the multi-scale framework of the stochastic pore structure including basic model assumptions is discussed. The generation algorithm of pore structure is presented in Section 3. To mimic closely the geometry of real porous materials by matching the statistical properties of real samples, such as the effective porosity and the pore surface, the shortest path and the clustering coefficient are performed in Section 4. Based on the MIP experiment, the algorithm validation for the reconstruction of pore structures is investigated in Section 5, in which the different distribution of the connection number is taken into account.

2 Multiscale represention of the pore structure

The pore-scale configurations of porous material are highly chaotic, consisting of a spatial network of pores in which larger pores are connected via narrower pores. In this paper spheres in the model represent larger pores with cylinders representing the connections (narrower pores) between them. Suppose that, in the porous material with random distribution of a large number of pores, there exists a constant ε satisfying the following condition: $0 < \varepsilon << L$, where L characterizes the macro scale of the investigated domain X. Thus, the porous material can be regarded as a set of periodic unit cells Y. That is, $X = \bigcup Y$, as shown in Fig. 2, where it is assumed that all unit cells Y have the same probability distribution ω of the spheres and cylinders of the same size ε. Thus, the probability distribution model of the investigated porous material can be prescribed by the probability distribution inside a statistic screen with ε-size, and the different values of ε have the different results in different length scale.

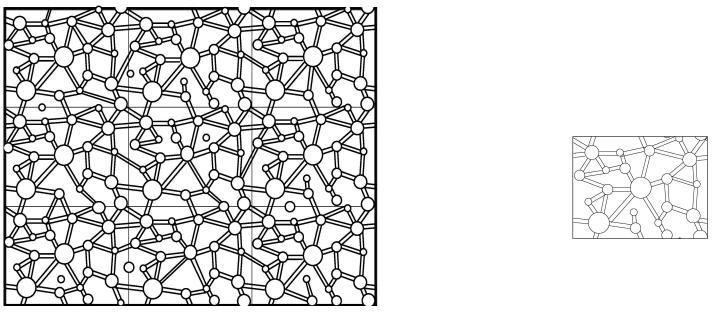

(a) Macro structure X (b) Representative unit cell Y

Figure 2: The macro structures with statistical periodic configuration and their unit cell

So we will mainly focus on the computer generation algorithm for a ε-statistic screen with random distribution of a large number of spheres and cylinders. The representation of the pore-scale network configurations for the porous material with random distribution of a large number of spheres and cylinders can be characterized as follows:

Firstly, the randomness of spheres is divided into two geometric ones: the shape of sphere, namely, its diameter, and the location of sphere, namely, its central coordinates. Secondly, the randomness of cylinder is represented by its shape which includes its diameter and length, while its location is determined by the location of its connected spheres.

Thus, the characteristic of random distribution of a plenty of pores in a ε screen can be represented by the probability density functions of 4 random parameters of spheres and 2 random parameters of cylinders: the shape parameters, namely, the diameter of sphere D_s, and the location parameters, namely, the central points (x_o, y_o, z_o) of the sphere, the diameter of cylinder D_c, and the length of cylinder L_c.

It is self-evident that in this paper only the 3-D computer generation method will be discussed below. Since the ε-statistics screen can be seen as a cube, we will discuss the 3-D computer generation method only on a cubic domain.

3 Stochastic reconstruction algorithm based on Monte Carlo method

In order to produce a pore-scale network model of porous material that resembles real porous material in the statistical sense, the random sampling principle of Monte Carlo simulation method is used. The model construction process consists of two main parts:

(1) An assembly of randomly distributed spheres will be arranged in the cube-shaped domain randomly. An arrangement of spheres is shown in Fig.3(a). The major factors to be considered are the size distribution and the spatial distribution of the spheres. An effective generation algorithm which falls into the category of take-and-place methods is considered below. In the take-and-place algorithm [Bažant, Tabbara, Kazemi, and Pijaudier-Cabot (1990); Schlangen and Mier (1992)], the generated spheres are filled into the cubic domain with rejection in such a way that there is no overlapping with spheres already placed. Considering the size and spatial position of the spheres, they can be constructed with four random parameters: The size parameters, i.e., the diameter D, and the location parameters, i.e., the central points (x_0, y_0, z_0) of the sphere. Moreover, the size parameters of the generated spheres satisfy the specified random distribution model to completely ensure the randomness of this parameter, and the location parameters can be temporarily considered

as a uniform random distribution.

(2) An assembly of randomly distributed cylinders which represent connections between the spheres, the major factors to be considered are the connection numbers, size and spatial position of the two adjacent spheres. Here, the connection numbers denote the number of connections.

In order to construct the algorithm suitable to several stochastic parameters, the lemma in [Gao (2003); Yu, Cui, and Han (2008)], namely, selection method lemma, is developed below.

Theorem1. Suppose that $\xi_1, \xi_2, \cdots, \xi_t, \eta_1, \eta_2, \cdots, \eta_t$ are independent random variables. $\xi_1, \xi_2, \cdots, \xi_t$ obey the uniform distributions on $(a_1, b_1), (a_2, b_2), \cdots, (a_t, b_t)$, and $\eta_1, \eta_2, \cdots, \eta_t$ all are random variables on (0,1), respectively. Furthermore, suppose that $f_1(x_1), f_2(x_2), \cdots, f_t(x_t)$ are the density functions on $(a_1, b_1), (a_2, b_2), \cdots, (a_t, b_t)$, and satisfy

$$\int_{a_1}^{b_1} f_1(x_1)dx_1, \int_{a_2}^{b_2} f_2(x_2)dx_2, \cdots, \int_{a_t}^{b_t} f_t(x_t)dx_t \tag{1}$$

Then, for any positive constants $\alpha_1, \alpha_2, \cdots, \alpha_t$, which satisfy $\alpha_1 f_1(x_1) \leq 1, \alpha_2 f_2(x_2) \leq 1, ..., \alpha_t f_t(x_t) \leq 1$ for $x_1 \in (a_1, b_1), x_2 \in (a_2, b_2), \cdots, x_t \in (a_t, b_t)$, one obtains

$$\begin{aligned} &P(\xi_1 \leq d_1, \xi_2 \leq d_2, \cdots, \xi_t \leq d_t \mid \alpha_1 f_1(\xi_1) \geq \eta_1, \alpha_2 f_2(\xi_2) \geq \eta_2, ..., \alpha_t f_t(\xi_t) \geq \eta_t) \\ &= \int_{a_1}^{d_1} f_1(x_1)dx_1 \int_{a_2}^{d_2} f_2(x_2)dx_2, \cdots, \int_{a_t}^{d_t} f_t(x_t)dx_t \\ &(a_1 \leq d_1 \leq b_1, a_2 \leq d_2 \leq b_2, \cdots, a_t \leq d_t \leq b_t) \end{aligned} \tag{2}$$

The stochastic parameters in our generation method is given based on Theorem 1.

3.1 Take-and-place method

The specified random distribution model is a certain given grading sphere-size distribution curve which is obtained from experiment or a known mathematical function. The random spheres are selected depending on the shape of the size distribution curve. The take-process and place-process are performed concurrently in the sense that a sphere generated by the take-process is immediately placed into the cube. They are conducted in a sequence starting with the largest size spheres, proceeding until the last sphere of the size range has been placed, and then repeating for successively smaller size spheres because it is generally easier to pack the spheres into the cube in this way. Hence, it is necessary to divide the grading curve

into segments and determine the volume of spheres and cylinders to be generated within each grading segment Fig. 3(b).

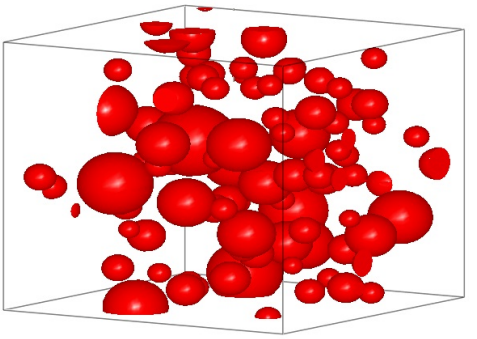

(a) An arrangement of spheres

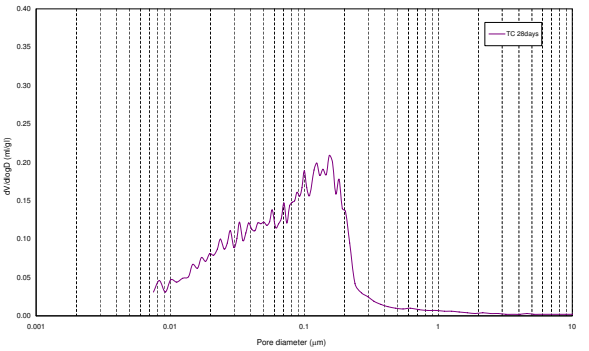

(b) Distribution curves of sphere sizes obtained from MIP

Figure 3: Stochastic arrangement of spheres and their grading size-distribution

The total volume of spheres and cylinders in each grading segment is normally given in terms of the volumetric ratio of them within per unit volume of porous material and the volume of the individual sphere and cylinder. Assume that, the grading curve is given by P(D) in which D is the diameter of the sphere and cylinder and P(D) is the distribution function of volume, $[D_i, D_{i+1}]$ is the grading segment. The volumetric ratio of each size spheres and cylinders can be obtained by dividing the given grading volume distribution curve. If the curve is closely represented by a known mathematical function, sphere and cylinder sizes are also randomly assigned according to the given distribution function by the same method. Then,

all the sphere and cylinder sizes recorded from the experiment analysis or a known mathematical function are numbered and ordered according to size.

The take-place-process starts with the grading segment containing the largest size spheres. For the grading segment $[D_i, D_{i+1}]$, the procedures are as follows:

(1) Calculating the volume of spheres and cylinders to be generated in the grading segment.

(2) Generating a random number defining the size of a sphere. Assuming that the size D has a uniform distribution between D_i and D_{i+1}, it may be taken as $D = D_i + \eta(D_{i+1} - D_i)$ in which η is a random number uniformly distributed between 0 and 1. Calculating the volume of the each generated sphere.

(3) Generating random numbers defining the location of a sphere and place the sphere into the cube as part of the place-process. The new sphere will be placed in a reasonable position so that the spheres in the cube are not overlapped with previously placed spheres.

(a) A Cartesian X-Y-Z coordinate system is used on the cube. During the take-process, the coordinates of the sphere generated are given in terms of local coordinates with respect to a reference point o inside the particle. When the sphere is placed into the cube, its position are defined by the X-Y-Z coordinates of the reference point o. Assuming a uniform probability distribution for the location of o throughout the cube area, the coordinates of o may be obtained as:

$$\begin{aligned} x_o &= X_{min} + \eta_1(X_{max} - X_{min}) \\ y_o &= Y_{min} + \eta_2(Y_{max} - Y_{min}) \\ z_o &= Z_{min} + \eta_3(Z_{max} - Z_{min}) \end{aligned} \tag{3}$$

where x_o, y_o and z_o are the coordinates of o, $X_{min}, X_{max}, Y_{min}, Y_{max}$ and Z_{min}, Z_{max} are the minimum and maximum X-, Y- and Z-coordinates of the cube area, and η_1, η_2 and η_3 are two independent random numbers uniformly distributed between 0 and 1.

(b) Check of overlapping can be done by determining whether the edge of the sphere intersects the edges of adjacent spheres.

(4) Generating cylinders using the method in the next subsection.

(5) Repeating steps (2)-(4) until the volume of the grading segment left to be generated is less than $\frac{\pi D_i^3}{6}$, i.e. not enough for generating another sphere. The

remaining area of sphere to be generated is then transferred to the generation of next grading segment.

(6) Repeating all the above steps for the next smaller size grading segment and then again for successively smaller size grading segments, until the last sphere of the smallest size has been generated and placed.

3.2 Cylinders generation method

In the generation method of cylinders, the connection number is the number of cylinders connected to one sphere, which reflects the whole spatial connectivity of all spheres in this model. The length of cylinders is obtained from the distance of two adjacent spheres and the size of cylinders satisfies the specified distribution. Since the layout of cylinders is dependent entirely on the distribution of the spheres, it need not be separately considered. The detailed progress is as follows:

(1) Generating a random integer number defining the connection number of each generated sphere, then recording them as c_n.

(2) For a sphere, searching all of its adjacent spheres whose distance is lower than a specified value d.

(3) If this sphere and one of the adjacent sphere c_n are bigger than zero, generating a cylinder and $\tilde{c}_n = c_n - 1$. It is proposed that the diameter D_c of cylinder between this two adjacent spheres is taken as μ times the smaller value of D_a and D_b, where μ is a random number uniformly distributed between 0 and 1, and D_a and D_b are the diameter of two adjacent spheres. The length of cylinders is the distance of the two adjacent spheres.

$$D_c = \mu min\{D_a, D_b\} \tag{4}$$

(4) Repeating all above steps for next sphere until all cylinders of the last sphere has been generated.

4 Evaluation of the expected pore characteristics for the generated pore-scale model

4.1 The effective porosity and pore surface

As for the porous materials with random pore-scale network stated previously, the expected pore characteristics, such as the effective porosity $\bar{P}$ and the effective pore surface $\bar{S}$, can be evaluated in the light of statistical meaning.

Suppose that the porosity and pore surface for a sample ω^s are $P(\omega^s)$ and $S(\omega^s)$. The procedures of the expected characteristics for random pore-network model can be computed as follows:

(1) Based on the statistical characteristic of the spheres and the cylinders for any random distributions ω^s, a pore-network sample is generated. Then evaluate the porosity and pore surface for a sample ω^s are $P(\omega^s)$ and $S(\omega^s)$ corresponding to sample ω^s.

(2) Generating M samples for any random distributions $\omega^s, s = 1, \cdots, M$ and from Kolmogorov strong law of large numbers, the expected pore characteristics, such as the effective porosity and the effective pore surface can be calculated in formula

$$\bar{P} = \lim_{M\to\infty} \frac{\sum_{s=1}^{M} P(\omega^s)}{M}, \quad \bar{S} = \lim_{M\to\infty} \frac{\sum_{s=1}^{M} S(\omega^s)}{M} \tag{5}$$

4.2 Shortest path and Clustering coefficient

The shortest path problem [Cherkassky, Goldberg, and Radzik (1996)] is the problem of finding a path between two vertices (or nodes) in a graph such that the sum of the weights of its constituent edges is minimized. The shortest path problem can be formally defined as follows: Given a weighted graph (that is, a set V of vertices, a set E of edges, and a real-valued weight function $f : E \to R$), and elements v and v' of V, find a path P from v to a v' of V so that $\sum_{p\in P} f(p)$ is minimal among all paths connecting v to v'.

The definition of the all-pairs shortest path problem is to find shortest paths between every pair of vertices v, v' in the graph. If the pore structure is represented as a graph where vertices describe pore chambers and edges describe pore throats, all-pairs shortest path algorithms can be used to find an optimal path of permeability. In this place, we use the Johnson's algorithm to compute the shortest path of the pore structure. Johnson's algorithm [Johnson (1977)] is a way to find the shortest paths between all pairs of vertices in a sparse directed graph.

Firstly, a definition of the reweighting function $\hat{w}(u,v) = w(u,v) + h(u) - h(v)$ is given. By reweighting, we have a new set of edge weights $\hat{w}$ which must satisfy two important properties.

(1) For all pairs of vertice u and v, a path p is a shortest path from u to v using weight function w if and only if p is also a shortest path from u to v using weight function $\hat{w}$.

(2) For all edges (u, v), the new weight $\hat{w}(u, v)$ is nonnegative.

So it does not change shortest paths, but reweight to a nonnegative value. Then, the algorithm consists of the following steps:

(1) Adds a new node with zero weight edge from it to all other nodes.

(2) For each node, we run the Bellman-Ford algorithm [Bellman (1958)] once.

(3) Reweight every edge to have all positive weight edges to use Dijkstra's algorithm [Dijkstra (1959)].

(4) Runs Dijkstra's algorithm on each node using reweighting function to find the shortest paths in the reweighted graph.

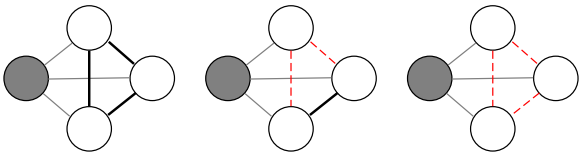

Figure 4: The clustering coefficient

The definition of the clustering coefficient (C_v) [Watts and Strogatz (1998)] is as follows: Suppose that a vertex v has k_v neighbors, then at most $k_v(k_v-1)/2$ edges can exist between them (this occurs when every neighbor of v is connected to every other neighbor of v). The clustering coefficient C_v of a vertex v measures what fraction of this set is actually connected Fig.4. For a large, completely random graph, C_v is $< k > /N$, while for a completely connected graph C_v is 1. The average of the local clustering coefficients of all the vertices n is defined as

$$\bar{C} = \frac{1}{n}\sum_{i=1}^{n} C_i, \tag{6}$$

Together with the shortest path, the clustering coefficient is implemented by Watts and Strogatz [Watts and Strogatz (1998)] as a measure of the "small world" property, and we have measured the unidirectional clustering coefficients.

To verify the above algorithm, several simulation results for 3-D domains are given in next section.

5 Numerical results and discussion

Since it is difficult to look inside the porous material to observe and experimentally determine the actual microscopic pore structure, effective reconstruction methods allow generation of realistic structures, and subsequent analysis can be performed to compute macroscopic properties. The above algorithm will be employed to generate several pore structure model based on some random distribution functions and MIP experiment. Then the algorithm will be applied to cubic section of the actual concrete, the key statistical characteristics of microscopic pore structure model will be compared with the results of Mercury injection experiment.

5.1 Reconstruction of pore structure based on random distribution functions

As described in the above model, the pore connection number is defined as the number of throats which attach to the different pore. This variable is stochastic and not easy to get direct measured so far. In the developed model, the mean pore connection number is taken as the stochastic variable obeyed some kind of distribution mathematically. In the following, two kinds of normally used distribution are employed to illustrate the developed method.

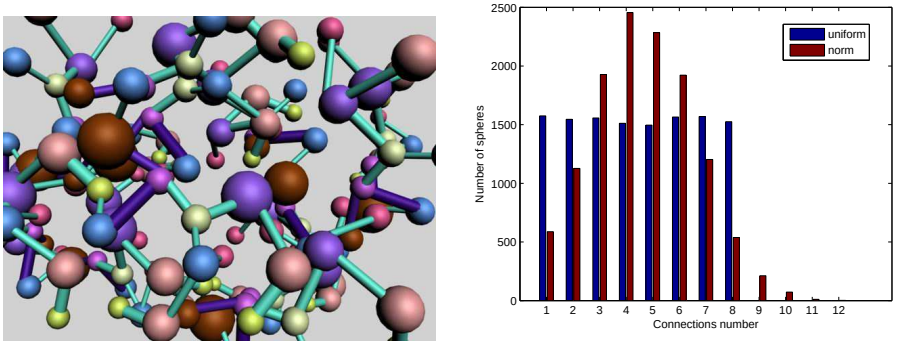

(a) (b)

Figure 5: (a) Pore structure; (b) Pore connection number

Test the algorithm on the ε-statistic screen which is a $1 \times 1 \times 1$ cubic domain, and different scale pore-scale network can be obtain from the different ε. The generated pore-network model is illustrated in Fig.5(a), the required total pore-network volume fraction is 20% and the central points (x_o, y_o, z_o) of spheres obey the uniform distribution in $[0,1] \times [0,1] \times [0,1]$. Then two different distribution of the connection number can be applied. One is that the connection number is controlled to

obey uniform distribution, where the mean connection number vary between 2 and 10. Another is that the connection number used for our test is controlled to obey norm distribution with the density function

$$f(x) = \frac{1}{\sqrt{2\pi}\sigma} e^{\frac{-(x-\mu)^2}{2\sigma^2}} \tag{7}$$

where is the mean and σ is the standard deviation of the mean. Fig.5(b) shows the computational results of the connection number, where the mean connection number is 4 and obeys the uniform and norm distribution.

After defining the distribution of mean connection number, the pore structure can thus be reconstructed. A unit cell with ε=1.0E-5 m is set to reconstruct the pore structure. Following the above methodology, a three dimensions pore structure of is illustrated. The minimum and maximum diameters of the spheres are 6.0E-3 μm and 2.67E-1 μm, where the diameters of the spheres and cylinders vary uniformly or obey the norm distribution (7). Fig.6 compares the number of the spheres and cylinders, where their diameter obey the different size distributions.

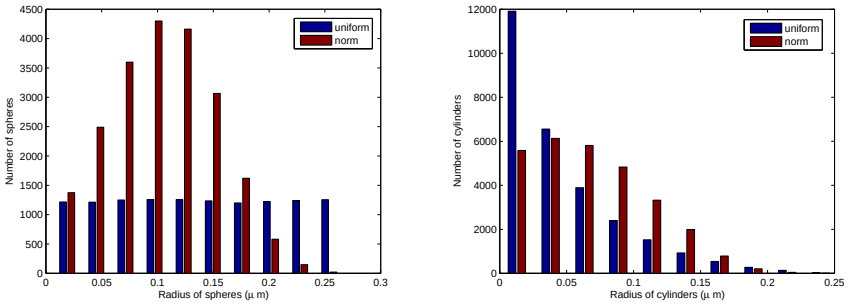

(a) (b)

Figure 6: (a) Number of spheres; (b) Number of cylinders for the different size distributions

5.2 Reconstruction of pore structure based on MIP experiment

As mentioned in Section 1, although many techniques are available to study the microstructure of porous materials, mercury intrusion porosimetry (MIP) is one of the most commonly-used techniques. It provides a fast method to obtain information about porosity and pore size distribution.

In this study, a typical cement paste is employed to get the pore information. The specimen is cured in 28 days after standard casting procedure and rotation [Ye

(2003)]. At the end of each curing period, the sample is removed and split into small pieces of about 1 cm^3. Then, the samples are placed into an oven at 105 ($^\circ C$). Water loss is monitored and recorded for 24 hours until weight stability is reached. The MIP measurement is performed with a PMI automated porosimeter. The maximum pressure of PMI automated porosimeter is 420 MPa. In order to avoid the influence of higher pressures damaging the CSH gel structure, the highest pressure used in this experiment is 212 MPa. According to Washburn's Equation[Washburn (1921)], this pressure can access the minimum pore diameter of 0.0069 μm.

5.2.1 Pore volume distribution

Pore structures based on experimental data are reconstructed and compared with the corresponding one of the experimental curves Fig.3(b). The normalized unity pore size distributions (PSD) in the form dV/dlogD = f(r) obtained from the experimental method, as well as the corresponding theoretical distribution dV/dlogD = f(r) obtained using the model, are shown in Fig.7. it should be emphasized that the different runnings of the Monte Carlo simulation produce similar but not quite identical dV/dlogD profiles. Those different fittings are practically identical at small D values but tend to differentiate from each other at larger values. Nevertheless they exhibit the same fine structure in the detailed distribution.

As is shown in the above sections, the criterion for the fitting of the developed pore network with the experimental observation is accurate and efficient. This is shown in Fig.7 where a very good fitting is indeed observed between the experimental data and the fitting line calculated from the model. We draw attention to the fact that this fitting of the model is a little abnormal in the bigger pores region for the moment. This mis-fitting is due to the fact that the simulation of most pores used discrete method whereas only a small percent of bigger pore region used the MIP methodology determined by the continuous plots, in other words, the model didn't accurately cover the bigger pore region. This is one of the weaknesses of the model.

5.2.2 The effective pore surface

From Fig.8, it is shown that the effective pore surface inside the test specimens decreases with the mean connection number, and the effective pore surface exhibits a slight increase in the end stage. Nevertheless, the effective pore surface vary from 31.6 to 33.4, it is obvious that this is only about 5%. This observation indicates that the change of the effective pore surface caused by different mean connection number is insignificant. It seems that more work should be done to trace this trend and estimation needs further efforts probably for the general application.

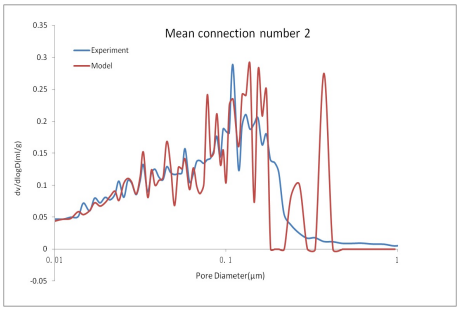

(a) Uniform distribution

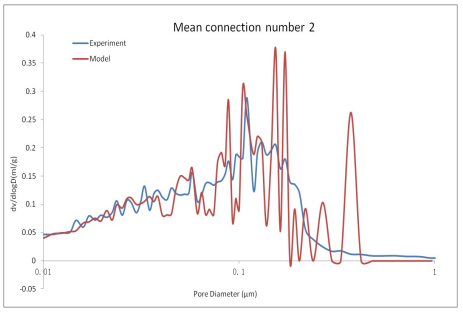

(b) Norm distribution

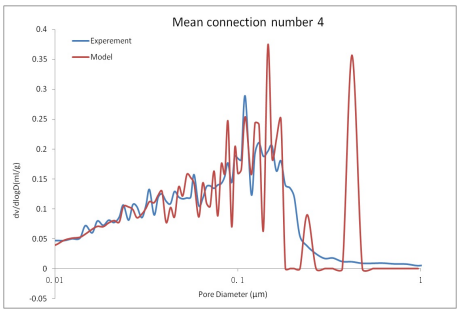

(c) Uniform distribution

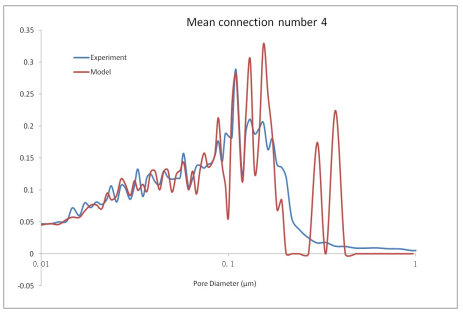

(d) Norm distribution

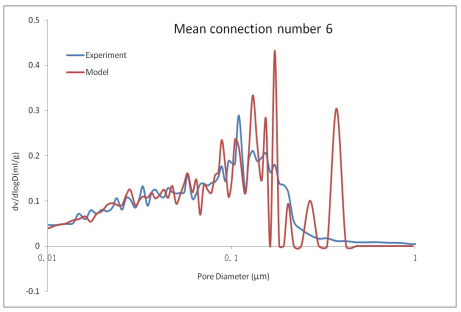

(e) Uniform distribution

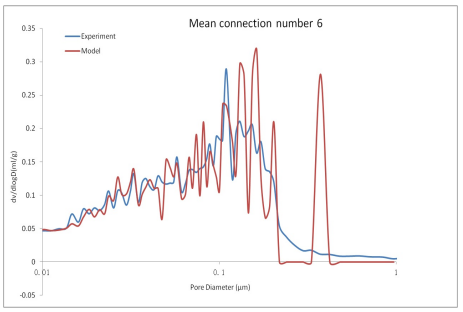

(f) Norm distribution

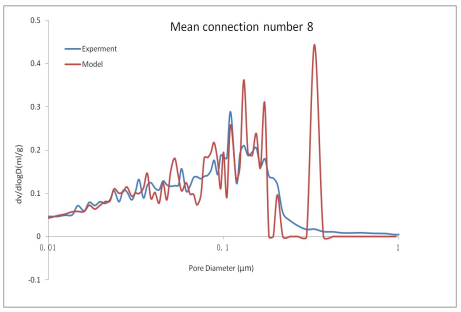

(g) Uniform distribution

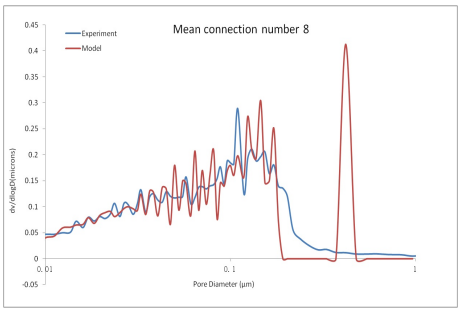

(h) Norm distribution

Figure 7: The eight different theoretical runnings of the Monte Carlo simulation: The normalized unity pore volume distribution (dV/dlogD)=f(r) obtained via the MIP method and the simulation are shown with the blue and the red solids.

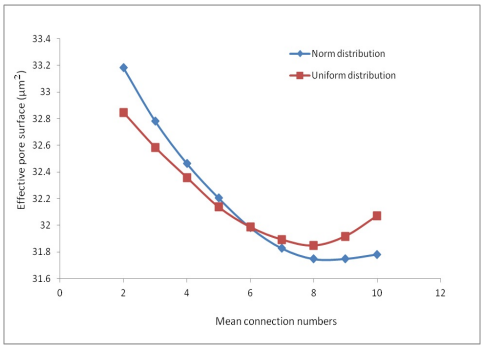

Figure 8: Influence of pore connection number on effective pore surface

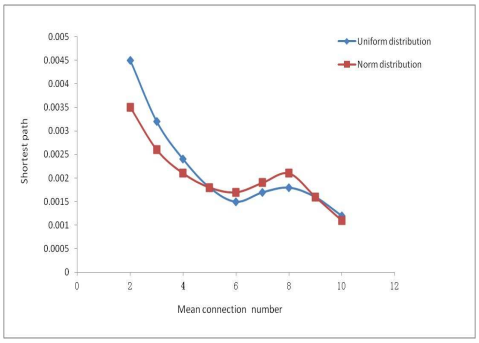

(a)

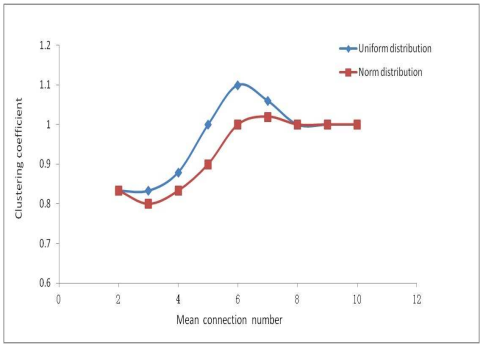

(b)

Figure 9: Influence of pore connection number on the shortest path and clustering coefficient

5.2.3 The shortest path and the clustering coefficient

Meanwhile, the shortest path and the mean local clustering coefficient was computed and the estimated values are in Fig.9. We observe that the shortest path decreases gradually with the increase of the mean connection numbers from 2 to 10 by two statistical distribution. The mean local clustering coefficient calculated using the Johnson's algorithm also keeps inalterability with the change of the mean connection numbers, in which a very good fitting is indeed observed that the present method can obtain corresponding connectivity with experiment. Nevertheless it seems that a more detailed discussion and explanation is needed for the moment, the more understanding and estimation needs further efforts probably from a much larger set of data. But the general trends traced in the present work should applied in general.

6 Conclusions

An effective computer generation algorithm for modeling the multiscale pore structures for porous materials is proposed in this paper. The model construction process consists of two main parts: the assemblies of randomly distributed spheres and cylinders. The spheres are generated with shapes following certain given grading size distribution curve which obtained from MIP experiment or a known mathematical function. The generation algorithm of the location parameters incorporates a take-and-place method and a selection algorithm. Especially for the selection algorithm, it can simulate not only the model with a uniformly random distribution, but also those with a special random distribution, and it can also be extended to simulate the mixed model of several random distributions.

In accordance with the connection numbers of each sphere, the cylinders are generated by diameters being the random numbers between 0 and the diameter of smaller sphere, and length can be determined by the distance of two adjacent spheres. Connection numbers are used for the study because they are a key step to provide a good connected pore structure. Future work will focus on using this pore structure to predict flow properties, such as relative permeability or diffusivity. The effectiveness of algorithm will be verified after these jobs.

Acknowledgement

The authors would like to thank the referees for their valuable suggestions and corrections, which contribute significantly to the improvement of the paper. This research was financially supported by the National Basic Research Program of China (973 Program: 2011CB013800), the National Natural Science Foundation of China, with Grant nos. 50908167, 11126132, and 50838004, and the Funda-

mental Research Funds for the Central Universities of China. The financial support of research is gratefully acknowledged.

References

Bažant, Z.; Tabbara, M.; Kazemi, M.; Pijaudier-Cabot, G. (1990): Random particle model for fracture of aggregate or fiber composites. *Journal of Engineering Mechanics*, vol. 116, no. 8, pp. 1686–1705.

Bellman, R. (1958): On a Routing Problem. *Quarterly of Applied Mathematics*, vol. 16, pp. 87–90.

Cherkassky, B.; Goldberg, A.; Radzik, T. (1996): Shortest paths algorithms: Theory and experimental evaluation. *Mathematical Programming*, vol. 73, pp. 129–174.

DeHoff, R. T.; Aigeltinger, E. H.; Craig, K. R. (1972): Experimental determination of the topological properties of three-dimensional microstructures. *Journal of Microscopy*, vol. 95, no. 1, pp. 69–91.

Dijkstra, E. (1959): A note on two problems in connexion with graphs. *Numerische Mathematik*, vol. 1, no. 1, pp. 269–271.

Dong, L.; Atluri, S. N. (2012): Development of 3d trefftz voronoi cells with ellipsoidal voids &/or elastic/rigid inclusions for micromechanical modeling of heterogeneous materials. *CMC: Computers, Materials & Continua*, vol. 30, pp. 39–82.

Dullien, F. A. L. (1979): *Porous media: Fluid transport and pore structure*. Academic Press.

Gao, H. X. (2003): *Statistical computation*. Peking University Press.

Garboczi, E. J.; Bentz, D. P. (1996): Modelling of the microstructure and transport properties of concrete. *Construction and Building Materials*, vol. 10, no. 5, pp. 293 – 300.

Han, F.; Cui, J.; Yu, Y. (2009): The statistical second-order two-scale method for thermomechanical properties of statistically inhomogeneous materials. *Computational Materials Science*, vol. 46, no. 3, pp. 654 – 659.

Han, F.; Cui, J.; Yu, Y. (2010): The statistical second-order two-scale method for mechanical properties of statistically inhomogeneous materials. *International Journal for Numerical Methods in Engineering*, vol. 84, no. 8, pp. 972–988.

Johnson, D. B. (1977): Efficient algorithms for shortest paths in sparse networks. *The Journal of the ACM*, vol. 24, no. 1, pp. 1–13.

Jr., D. S.; Sladek, V.; Sladek, J.; Zmindak, M.; Medvecky, S. (2012): Porous media analysis by modified mlpg formulations. *CMC: Computers, Materials & Continua*, vol. 27, pp. 101–127.

Liu, X. (2006): *Microstructural investigation of self-compacting concrete and high-performance concrete during hydration and after exposure to high temperatures*. PhD thesis, Ghent University, 2006.

Liu, X.; Zeiml, M.; Lackner, R.; Mang, H. A. (2010): Upscaling of permeability of porous materials: First insight into the effect of pore-space characteristics. *International Journal for Multiscale Computational Engineering*, vol. 8, no. 1, pp. 103–112.

Mata, V. G.; Lopes, J. C. B.; Dias, M. M. (2001): Porous media characterization using mercury porosimetry simulation. 1. description of the simulator and its sensitivity to model parameters. *Industrial & Engineering Chemistry Research*, vol. 40, no. 16, pp. 3511–3522.

Sadouki, H.; Mier, J. G. M. (1997): Meso-level analysis of moisture flow in cement composites using a lattice-type approach. *Materials and Structures*, vol. 30, pp. 579–587.

Schlangen, E.; Mier, J. G. M. (1992): Simple lattice model for numerical simulation of fracture of concrete materials and structures. *Materials and Structures*, vol. 25, pp. 534–542.

Tsakiroglou, C. D.; Payatakes, A. C. (1998): Mercury intrusion and retraction in model porous media. *Advances in Colloid and Interface Science*, vol. 75, no. 3, pp. 215 – 253.

Underwood, E. E. (1970): *Quantitative stereology*. Addison-Wesley.

Washburn, E. W. (1921): The dynamics of capillary flow. *Phys. Rev.*, vol. 17, pp. 273–283.

Watts, D. J.; Strogatz, S. H. (1998): Collective dynamics of s̀mall-worldńetworks. *Nature*, vol. 393, pp. 440–442.

Yan, Z. Y.; Zhang, J.; Ye, W.; Yu, T. X. (2010): Numerical characterization of porous solids and performance evaluation of theoretical models via the precorrected-fft accelerated bem. *CMES: Computer Modeling in Engineering & Sciences*, vol. 55, pp. 33–60.

Yang, Z. Q.; Cui, J. Z.; Nie, Y. F.; Ma, Q. (2012): The second-order two-scale method for heat transfer performances of periodic porous materials with interior surface radiation. *CMES: Computer Modeling in Engineering & Sciences*, vol. 88, pp. 419–442.

Ye, G. (2003): *Experimental study and numerical simulation of the development of the microstructure and permeability of cementitious materials*. PhD thesis, Delft University of technology, 2003.

Ye, G.; Lura, P.; Breugel, K. (2006): Modelling of water permeability in cementitious materials. *Materials and Structures*, vol. 39, pp. 877–885.

Yu, Y.; Cui, J.; Han, F. (2008): An effective computer generation method for the composites with random distribution of large numbers of heterogeneous grains. *Composites Science and Technology*, vol. 68, no. 12, pp. 2543 – 2550.

Zeiml, M. (2008): *Concrete subjected to fire loading-from experimental investigation of spalling and mass-transport properties to structural safety assessment of tunnel linings under fire*. PhD thesis, Vienna University of Technology, 2008.